

## DESIGN OF METAPARTICLES AS SHARP FREQUENCY-SELECTIVE OBSCURANT AEROSOLS

Sharhabeel Alyones<sup>1, 2, \*</sup>, Al V. Jelinek<sup>1</sup>, Michael Granado<sup>1</sup>, and Charles W. Bruce<sup>1</sup>

<sup>1</sup>Physics Department, New Mexico State University, Las Cruces, NM 88003, USA

<sup>2</sup>Physics Department, Hashemite University, Zarqa 13115, Jordan

**Abstract**—In this article, artificial aerosol metaparticles are investigated. These particles are based on interacting single split rectangular resonators (SRRs) imprinted on a one-sided thin dielectric substrate. These particles produce sharper transmission bandstops with adjustable bandwidths compared to conventional artificial aerosol obscurants like fibers, spheres, discs. The particle design is performed in the microwave region with the intention to be scalable to the infrared. Particles with couplings between two, three, and four SRRs are introduced. Numerical simulations and experimental measurements of the transmission parameter of the particles are introduced and compared with fibrous aerosols. These particles may be used as good electromagnetic obscurants in the atmosphere.

### 1. INTRODUCTION

Small aerosol particles that can block one or more portions and allow passage of the rest of an electromagnetic frequency band are of interest for electromagnetic shielding and obscurant application. A sharp-edged transmission bandstop is in demand where excellent out of band transmission is desired. Metallic fiber — like particles are good candidates and have been studied extensively, both numerically and experimentally [1–5]. While fibrous aerosols are considered to be relatively sharp resonators, their behavior is not as sharp as desired. Furthermore, the bandwidth of the fiber resonance is not adjustable.

Negative refractive index metamaterials (NRM) were theoretically predicted by Vesalogo [6]. NRM have novel electromagnetic structures

---

*Received 7 February 2013, Accepted 9 April 2013, Scheduled 17 April 2013*

\* Corresponding author: Sharhabeel Alyones (salyones@hu.edu.jo).

that exhibit extraordinary electromagnetic properties compared with ordinary materials. These extraordinary properties make them suitable for various electromagnetic applications that are not achievable by ordinary materials. Negative refraction, invisible metals, magnetic mirrors, cloaking, and filtering are some examples of these applications [6–10]. Planar metamaterials that consist of broad-side, asymmetric, single split rectangular ring resonator (aSRR) imprinted on a thin dielectric substrate have shown sharp bandstop behavior located at a central frequency that depends on the size of the resonator. This behavior is due to the presence of a trapped mode current that is excited through weak free-space coupling and asymmetry is a required condition for this behavior. The resonance is due to the electric field excitation [11,12]. Edge-on planar metamaterials that consist of concentric split rectangular ring resonators (SRRs) have also shown sharp bandstop behavior due to the magnetic resonance of the resonator while asymmetry is not required here. Various aspects of edge-on planar SRRs have been studied numerically and experimentally [13–16].

Microstrip line electronic elements based on coupled SRRs, which produce wide and sharp bandstop/bandpass filters, have been designed in many previous research articles, see for example [17]. Rectangular wave guide bandstop filters using three adjacent SRRs have been introduced in [18,19]. The designs in [18] and [19] produce a wide bandstop. The bandstop does not have sharp edges as desired for an obscurant particle and there is no procedure to adjust the bandwidth, as this procedure is also important for practical obscurant applications.

In this article, a releasable metamaterial aerosol particle based on interacting SRRs is constructed. The performance of two, three and four edge-on interacting single SRRs in terms of their  $S$ -parameters is introduced numerically and experimentally. The purpose is to design a particle that produces a sharp-edged and adjustable bandstop in the microwave wavelength region that is scalable to the short wavelength region. The electromagnetic behavior scales throughout the Drude domain, which includes the infrared and microwave limits. Although, as an aerosol, a sharp-edged orientational average response is desired, this investigation focuses on the response at edge-on incidence.

The rest of the paper is organized as follows: in Section 2, the fabrication, measurement procedure and numerical simulation model are presented. In Section 3, the transmission parameter  $S_{21}$  of two coupled SRRs is introduced numerically and experimentally. In Section 4, we introduce three and four coupled SRR particles that produce wider and sharper bandstops. In Section 5, comparison with fibrous aerosols obscurants is discussed; finally, conclusions are

introduced in Section 6.

## 2. MEASUREMENTS AND NUMERICAL SIMULATION PROCEDURE

The measurements were made using a low-dispersive, TEM transmission line which retains this character over a range of frequencies well beyond the boundaries of the measurements reported. The resonators were fabricated using positively-coated, lossy FR-4 circuit boards. The positively-coated boards provide a planar conductive pattern for the portion of the board that is not exposed to UV light following development and etching. The resonator masks were drawn to specification using 2D CAD software, and then printed on transparency film with a high resolution printer at 1200 dpi. The circuit board and resonator mask were sandwiched between two panes of glass and exposed to UV light. Once developed, the area exposed to the light is etched away and only the resonator is left in copper. However the etching process is not always precise and can leave the SSRs with dimensions that are slightly above or below the desired specifications for a given frequency. This change in size will cause a shift in frequency of the measured value as compared to simulated data of the precise dimensions. To achieve measurement results in close comparison with the theory, the resonators were photographed through a microscope and the dimensions of the resonators were determined after etching. Finally, dimensions were averaged and the computations were performed on these bases.

The numerical simulations were performed using the frequency domain formulation of the CST microwave studio simulator [20]. The particle was inserted at the center of a single mode rectangular waveguide with the top and bottom walls assigned a PEC boundary condition, while the sides were assigned a PMC boundary condition. This will ensure the magnetic field to be perpendicular to the resonators plane, as shown in Figure 1.

## 3. BANDSTOP PARTICLE USING TWO COUPLED SRRs

Figure 1 shows a single copper SRR imprinted on a loss-free FR-4 dielectric substrate of thickness 0.793 mm and electric permittivity 4.3. The thickness of copper cladding is 32  $\mu\text{m}$ . The dimensions of the resonator are chosen to operate in the C-band. When excited by an electromagnetic field with orientation as given in Figure 1, the magnetic resonance, a sharp bandstop at central frequency, is obtained as shown in Figure 2(a). The location of the central resonance

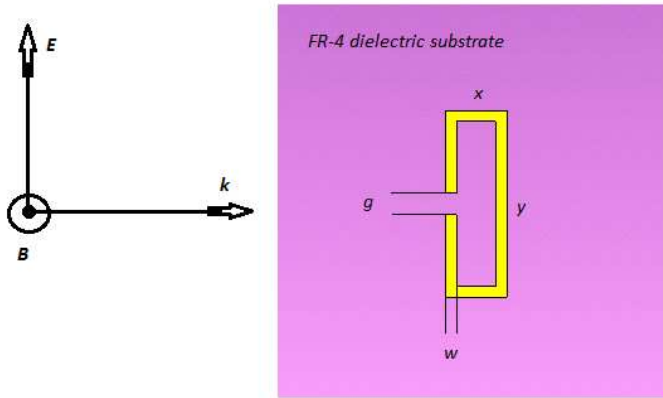


**Figure 1.** Single SRR with dimensions ( $y = 8.6$  mm,  $x = 2.8$  mm,  $g = 1$  mm,  $w = 0.5$  mm) imprinted on a FR-4 loss-free dielectric substrate and excited by a plane electromagnetic wave.

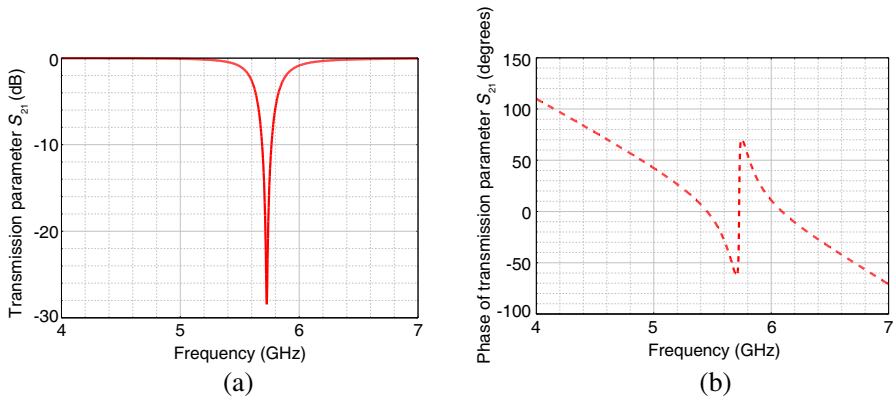


**Figure 2.** Simulated transmission parameter  $S_{21}$  (amplitude and phase) as a function of frequency for a single SRR as in Figure 1.

frequency depends on the size of the SRR. The SRR can be modeled as a simple LC circuit with resonance frequency:  $\omega_0 = \sqrt{1/LC}$ , where  $L$  and  $C$  are the effective inductance and capacitance of the SRR respectively. When a time varying magnetic field perpendicular to plane of the SRR is applied, a circulating current is induced according to Faraday's law. The phase of the  $S_{21}$  parameter is shown in Figure 2(b).

Next, a particle which consists of two identical SRRs imprinted on the FR-4 loss-free substrate is analyzed. Two designs are introduced

here: (a) the two gaps of the SRRs are in the same side (b) the two gaps are in the opposite sides, see Figure 3. The dimensions of each SRR are the same as in Figure 1. Figure 3 shows the simulated transmission parameter  $S_{21}$  as a function of frequency for different separations between the resonators. As we see from Figure 3, the interaction between the two resonators produces two resonance bandstops, the location and amplitudes of these stops depend on separation distance. The interaction between the resonators also depends on the relative orientation of the gaps. For the orientation in (a) we see that the lower frequency stop edge is sharper, while for the orientation in (b), the upper frequency bandstop edge is sharper. For specific separation distances, a somewhat wide bandstop is obtained with excellent out of band transmission in one side of the band and greatly reduced transmission on the other side depending on the orientation of the

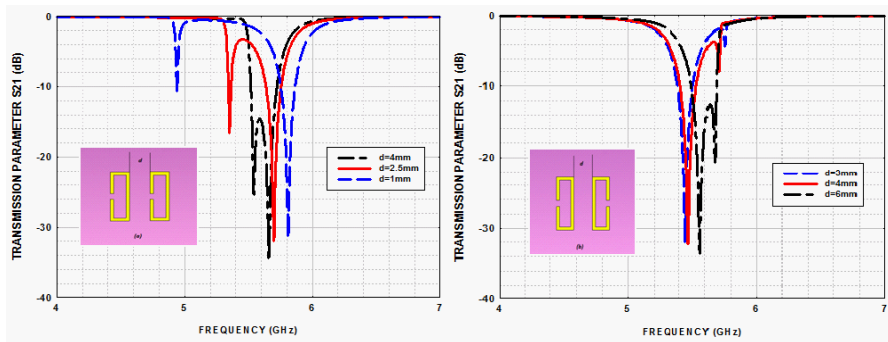


**Figure 3.** Simulated  $S_{21}$  parameter versus frequency for two coupled SRRs with different separation distances ( $d$ ) imprinted on a loss-free FR-4 dielectric substrate.

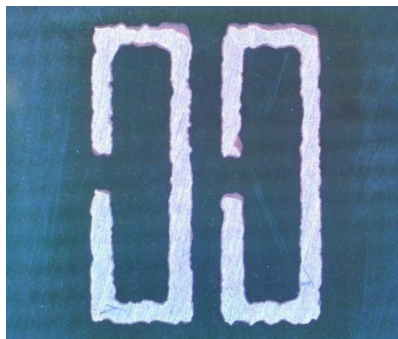


**Figure 4.** Microscope picture of the fabricated measured sample of two coupled SRRs.

gaps.

The designs in Figure 3 have been verified experimentally for various separation distances. Next we show an example of two SRRs imprinted on a lossy FR-4 substrate. The fabricated sample picture is shown in Figure 4. The proposed dimensions of each resonator are the same as those in Figure 1 with separation distance of  $d = 1$  mm, but due to the etching problems the dimensions came out slightly different, so, as we indicated earlier, the simulation here is for the fabricated sample not the proposed one. Figure 5(a) shows the simulation and measurement of  $S_{21}$  of the fabricated sample in Figure 4, the corresponding loss-free substrate calculation is also included. Good agreement between the simulation and measurement is achieved. The corresponding phase of the  $S_{21}$  parameter is shown in Figure 5(b).

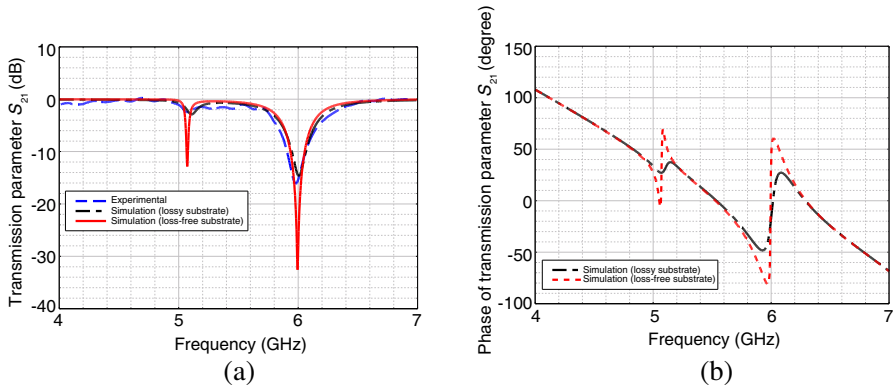


**Figure 5.** Simulated and measured  $S_{21}$  parameter (amplitude and phase) for the two coupled SRRs of Figure 4.

The coupling between two SRRs can be understood as follows; when two adjacent SRRs are excited by the incident electromagnetic field a bright LC resonant mode is induced by each SRR. When these two identical bright modes hybridize, the bright resonance mode splits into a low energy (frequency) resonance and a high energy (frequency) resonance leaving a relative transparency window in between. The size of the transparency window and location of the low and high energy resonances depend on the separation distance between the two SRRs (i.e., the strength of coupling). As the SRRs get closer to each other, the transparency window becomes wider and stronger in amplitude due to strong coupling. This coupling is similar to the phenomena of electrically induced transparency (EIT) [21]. The surface current distribution at the low and high energy modes are shown in Figure 6, for which a separation distance of  $d = 3$  mm is chosen. The currents

are out of phase for the low energy mode and in phase for the high energy mode. A stronger and broader high energy mode compared with low energy mode is achieved when the gaps are on the same side, and a stronger and broader low energy mode is achieved when the gaps are on opposite sides.

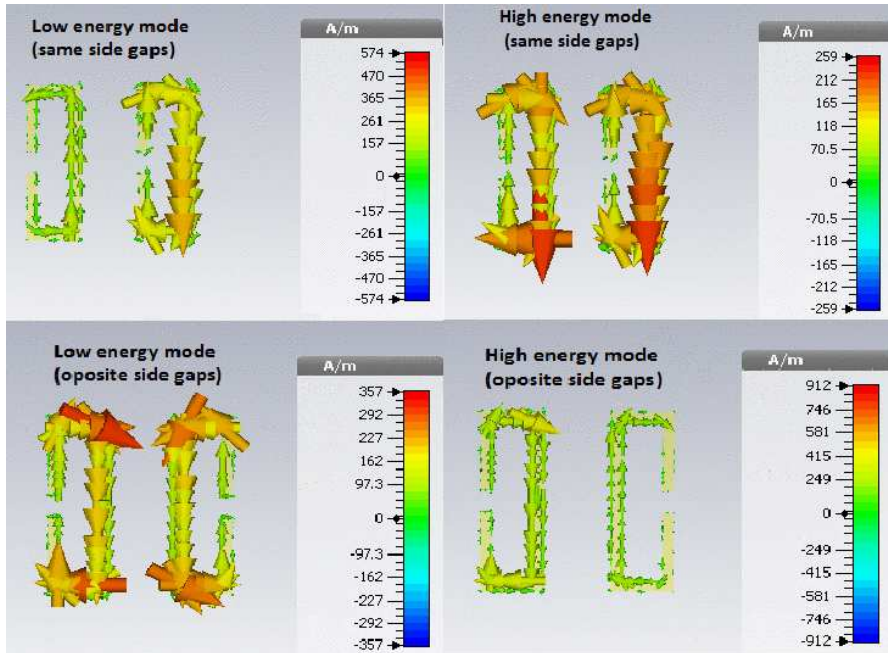


**Figure 6.** Top view of surface current distribution of two coupled SRRs for the same side gap and opposite side gap orientations.

#### 4. WIDER AND SHARPER BANDSTOPS USING THREE AND FOUR COUPLED SRRs

In Section 2, we have shown that one can produce a bandstop using two coupled SRRs by choosing an appropriate separation distance between them. The bandstop is limited in width and is relatively sharp on only one side depending on the orientation of the gaps.

To produce a wider bandstop with excellent out of band transmission on both sides we can use the behavior in Section 2. We couple two resonators, as in Figure 3(a), with a third resonator of a different size and with an opposing gap. This proposed particle is shown in Figure 7(a). The corresponding microscope picture of the fabricated particle is shown in Figure 7(b).

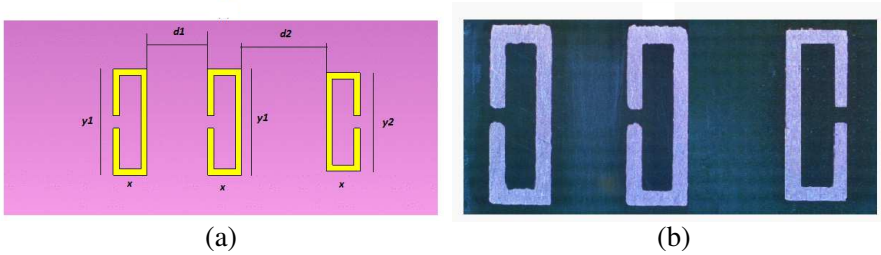


**Figure 7.** Three coupled SRRs imprinted on a loss-free FR-4 dielectric substrate,  $y_1 = 8.6$  mm,  $y_2 = 8.2$  mm,  $d_1 = 4$  mm,  $d_2 = 6.5$ . All other parameters are the same as in Figure 1. (a) Proposed particle, (b) fabricated particle (on a different scale).

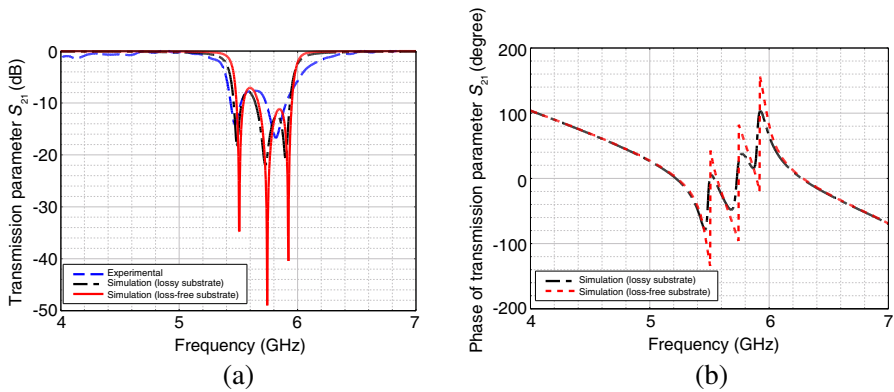


**Figure 8.** Simulated and measured transmission parameter  $S_{21}$  (amplitude and phase) for the three coupled SRRs in Figure 7.

Figure 8(a) shows the simulated transmission parameter  $S_{21}$  of the particle in Figure 7. The distances  $d_1$  and  $d_2$  were chosen through the swap feature of the CST MICROWAVE STUDIO to produce the best wider and sharper bandstop. We see that using three resonators with the orientation of Figure 7, a wider bandwidth is obtained with excellent out of band transmission on both sides ... if a loss-free substrate is used. The fractional bandwidth calculated at  $-3$  dB transmission is  $6.4\%$  for the loss-free substrate. Figure 8(b) shows the corresponding phase of the  $S_{21}$  parameter.

An even better design that can produce a much wider bandstop with a sharper band edge on both sides can be achieved using four SRRs. This fabricated design is shown in Figure 9. In this design we coupled two resonators like the system of Figure 3(a) with another two resonators like the system of Figure 3(b). Each of the two coupled

systems will produce an excellent band edge on one of the two sides of the bandstop; of course the sizes of the two subsystems should be different and chosen through the swap feature of CST. For the following presentation the distances  $d_2$  and  $d_3$  were chosen to obtain the best sharpness for the net bandstop filter. Figure 10 shows good agreement between the simulation and the experimental results for the lossy substrate. A much wider and sharper bandstop can be seen in Figure 10 with a fractional bandwidth of 13% at  $-3$  dB transmission for the loss-free substrate.

### 5. COMPARISON WITH FIBROUS ARESOLS OBSCURANTS

To compare the proposed metaparticles with fibrous aerosol particles, the natural logarithm of the inverse of the transmission parameter of Figure 10, with a loss free base substrate, is plotted and compared with

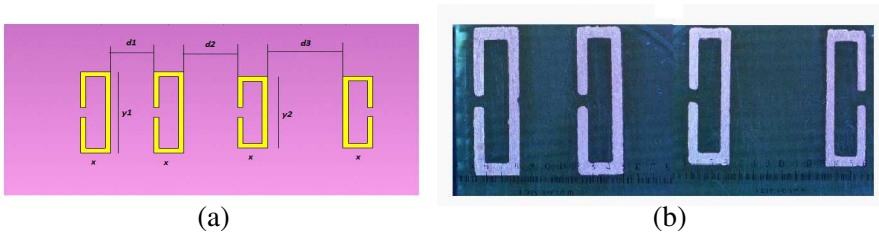


**Figure 9.** Four coupled SRRs imprinted on a lossy FR-4 substrate,  $y_1 = 9.6$  mm,  $y_2 = 8.6$  mm,  $d_1 = 4$  mm,  $d_2 = 5$  mm,  $d_3 = 7$  mm. All other dimensions as in Figure 1. (a) Proposed particle, (b) fabricated particle.

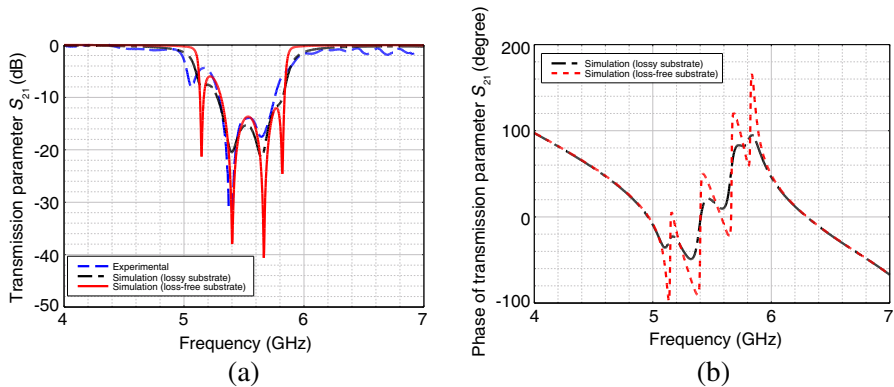


**Figure 10.** Transmission parameter  $S_{21}$  (amplitude and phase) of the four coupled ring resonators of Figure 9.

the extinction cross section of a copper fiber with length 26 mm and diameter of 30  $\mu\text{m}$ , with the  $E$ -field along the fiber axis [1, 2, 5]. The geometrical parameters of the fiber were chosen to produce the first resonant at 5.5 GHz. The results are shown in Figure 11. Figure 11(a) shows  $\ln(1/|S_{21}|)$  for the four coupled SRRs particle and Figure 11(b) shows the extinction cross section for the copper fiber. For the fiber, the extinction cross section is proportional to  $\ln(1/|S_{21}|)$ . As we see, it is clear that a much sharper bandstop is achieved using the metamaterials compared with the fiber, Furthermore the size of bandwidth is adjustable for the metamaterials by adding more SRRs, while this cannot be achieved using fibrous aerosols.

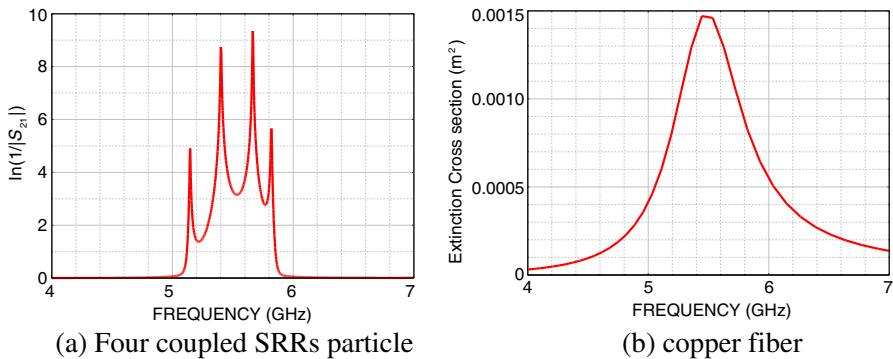


**Figure 11.** (a)  $\ln(1/|S_{21}|)$  (four SRRs particle) and (b) extinction cross section (copper fiber) versus frequency.

## 6. CONCLUSIONS

After a systematic review of designs, several aerosol particles have been introduced in this article to produce a single bandstop in the electromagnetic microwave c-band, and these wavelength-scalable designs are based on the coupling of SRRs. The bandstops have different widths and sharp cut-off edge on one side using the double SRR coupling. For the three- or four-SRR coupling, the sharp edge appears on both sides and almost a perfect wider sharp-edged bandstop is achieved using four SRRs. These particles are good candidates for electromagnetic shielding and obscurant applications when loss-free substrates are used. The designs have been verified experimentally, and good agreement is achieved between numerical calculations and experimental measurements in the case of lossy substrate base. In comparison to fiber-like particles, these metamaterials produce a much sharper and adjustable bandstop.

Finally, using this design procedure we see that there is no limitation on the bandwidth as one can couple more resonators to produce much wider bandstop by alternating coupling between two SRRs with gaps in the same side and another one with gaps on the opposite sides. This procedure of SRRs cascading, that ensures production of sharp edges and adjustable bandstop width is important for practical applications.

## ACKNOWLEDGMENT

The authors acknowledge the support of Mr. Jeff Hale at the Edgewood Chemical and Biological Center, U.S. Army, through contract # W911SR-11-C-0041 and for numerous related discussions.

## REFERENCES

1. Alyones, S., C. W. Bruce, and A. K. Buin, "Numerical methods for solving the problem of electromagnetic scattering by a finite thin conducting fiber," *IEEE Trans. Antennas Propag.*, Vol. 55, 1856–1861, 2007.
2. Bruce, C. W. and S. Alyones, "Visible and infrared optical properties of stacked cone graphitic microtubes," *Appl. Opt.*, Vol. 51, No. 16, Jun. 2012.
3. Alyones, S. and C. W. Bruce, "Electromagnetic scattering by finite conducting fiber: Limitation of a previous published code," *Journal of Electromagnetic Waves and Applications*, Vol. 25, No. 7, 1021–1030, 2011.
4. Bruce, C. W. and S. Alyones, "Extinction efficiencies for metallic fibers in the infrared," *Appl. Opt.*, Vol. 48, 5095–5098, 2009.
5. Bruce, C. W., A. V. Jelinek, S. Wu, S. Alyones, and Q. S. Wang, "Millimeter-wavelength investigation of fibrous aerosol absorption and scattering properties," *Appl. Opt.*, Vol. 43, 6648–6655, 2004.
6. Velasgo, V. G., "The electrodynamics of substances with simultaneously negative values of epsilon and mu," *Sov. Phys. Uspekhi*, Vol. 10, 1968.
7. Pendry, J. B., A. Holden, D. Robbins, and W. Stewart, "Magnetism from conductors and enhanced nonlinear phenomena," *IEEE Trans. Microwave Theory Tech.*, Vol. 47, 1999.
8. Simons, R. N., *Coplaner Waveguide Circuits, Components, and Systems*, Wiley-IEEE Press, 2001.
9. Wolff, I., *Coplanar Microwave Integrated Circuits*, Wiley-Interscience, 2006.

10. Shelby, R. A., D. R. Smith, and S. Schultz, "Experimental verification of a negative index of refraction," *Science*, Vol. 292, 77–79, Apr. 2001.
11. AL-Naib, I. A. I., C. Jansen, and M. Koch, "High Q-factor metasurfaces based on miniaturized asymmetric single split resonator," *Appl. Phys. Lett.*, Vol. 94, 2009.
12. Fedotov, V. A., M. Rose, S. L. Prosvirnin, N. Papasimakis, and N. I. Zheludev, "Sharp trapped resonances in planar metamaterials with a broken structural symmetry," *Phys. Rev. Lett.*, Vol. 99, 2007.
13. Elwi, T. A., "A further investigation on the performance of the broadside coupled rectangular split ring resonators," *Progress In Electromagnetic Research Letters*, Vol. 34, 1–8, 2012.
14. Penciu, R. S., K. Aydin, M. Kafesaki, T. Koschny, E. Ozbay, E. N. Economou, and C. M. Soukoulis, "Multigap individual and coupled split-ring resonator structures," *Optical Society of America*, Vol. 16, No. 22, 1–14, Oct. 2008.
15. Marques, R., F. Mesa, J. Martel, and F. Medina, "Comparative analysis of edge- and broadside-coupled split ring resonators for metamaterial design theory and experiments," *IEEE Trans. Antennas Propag.*, Vol. 51, No. 10, 33–41, Oct. 2003.
16. Balmaz, P. G. and O. J. F. Martin, "Electromagnetic resonances in individual and coupled split-ring resonators," *J. Appl. Phys.*, Vol. 92, No. 5, 2929–2936, Jun. 2002.
17. Hong, J. S. and M. J. Lancaster, "Design of highly selective microstrip bandpass filters with a single pair of attenuation poles at finite frequencies," *IEEE Trans. Microwave Theory Tech.*, Vol. 40, No. 7, 2000.
18. Shelkownikov, A. and D. Budimir, "Left-handed rectangular waveguide bandstop filters," *Microwave and Optical Technology Letters*, Vol. 48, 2006.
19. Rigi-Tamandani, A., J. Ahmadi-Shokouh, and S. Tavakoli, "Wideband planar split ring resonator based metamaterials," *Progress In Electromagnetic Research M*, Vol. 28, 115–128, 2013.
20. CST microwave studio, Sonnet Software, Inc., <http://www.CST.com>.
21. Jin, X., J. Park, H. Zheng, S. Lee, Y. Lee, J. Rhee, K. Kim, H. S. Cheong, and W. Jang, "Highly-dispersive transparency at the optical frequencies in planar metamaterials based on two-bright-mode coupling," *Optics Express*, Vol. 19, 22, 2011.